

LIGHT SCATTERING STUDY OF GELATION PROCESS OF FIBRIN GEL

Kenji Kubota, Atsuo Takahashi*, Rio Kita*, and Makoto Kaibara*

Faculty of Engineering, Gunma University, Kiryu, Gunma 376-8518, Japan

Fax: 81-277-30-1447, e-mail: kkubota@bce.gunma-u.ac.jp

*The Institute of Physical and Chemical Research (RIKEN), Wako, Saitama 351-0198, Japan

Fax: 81-48-467-9389, e-mail: ataka@postman.riken.go.jp

Gelation process of fibrinogen induced by the enzymatic action of serine protease, thrombin, was investigated by means of light scattering measurement and real space observation using confocal laser scanning microscopy (CLSM) focusing on the fractal nature of the fibrin gel network structure. It has been ascertained that light scattering measurement is able to characterize the gelation process and the growth kinetics. Stepwise gelation process, formation of fibrin monomers and protofibrils followed by the lateral aggregation to form fibrin fibers and gel network, was clearly demonstrated. At the gelation point, correlation function exhibited a power law behavior suggesting the self-similar nature of temporal fluctuation. Fractal dimension was evaluated from power law behavior based on the Muthukumar and Martin theory, which is originally conducted to the gel network consisting of flexible polymers. In order to examine those validity, CLSM was applied and 3-D network structure was reconstructed from the slice images. Two length scales characterizing the network structure were evaluated quantitatively. Box counting and power spectra by 3-D fourier transform of the real space images afforded the fractal dimension. Evaluated fractal dimensions are in good agreement with those obtained by light scattering.

Key words: Fibrinogen, Gel Network, Fractal Dimension, Light Scattering, Confocal Laser Scanning Microscopy

1. INTRODUCTION

Fibrinogen is a rod shaped protein with the molecular weight of 3.4×10^5 , and assembles into a three-dimensional gel network by the action of thrombin through the removal of fibrinopeptide A and B. Recent light scattering investigation ascertained clearly that the formation of fibrin gel proceeds in a stepwise manner: activation of fibrinogen to originate the fibrin monomer and end-to-end staggered polymerization of fibrin monomers (protofibril formation) in the first step, and a side-by-side association of protofibrils (fiber growth) resulting the gel formation in the succeeding step. [1,2,3] Approaching the gelation point, decay time distribution of the density fluctuation becomes so broad with shifting to longer time region, and the correlation function shows very slow decaying behavior corresponding to the growth of network structure. As a result, at the gelation point a self-similar decaying behavior in time scale is accomplished due to the hierarchy of fluctuation modes corresponding to a variety of spatial network structure. Thus, the power law behavior of the correlation function is realized, which means the nonexistence of the characteristic time. Sol-to-gel transition is the transition of connectivity and has been treated in terms of percolation model. [4] Percolated clusters have a spatially self-similar nature and its characteristics are expressed by the fractal one. Assuming the equality between the space and time self-similarities, the fractal nature of the gel could be characterized either by the time or by the spatial observations. Muthukumar et al presented the formulation of the fractal dimension for the flexible Rouse chain. [5,6] Since gel is a macroscopically large network connected with chains having various lengths, his formulation could be applied for the characterization of the fibrin gel, even though the fibrin gel consists of

stiff fibrin fibers. [3] In order to clarify this equality, direct and real space observations of the gel network is desirable. Of course, in situ observation in a hydrated state is necessary to rule out the possible artifacts. Confocal laser scanning microscopy (CLSM) is suitable one for this purpose. [7,8] Since fibrin fibers constructing the gel network have relatively thick diameters, they are visible by virtue of fluorescent probe.

In the present paper, we report the investigations of light scattering and CLSM studies of fibrin gel formation. 3-D network image was reconstructed from the sliced images. Fractal dimension of the gel network was evaluated by several procedures: power law behavior of the correlation function, box counting of 3-D images [9], power spectra by 3-D fourier transform [10], and the model fitting to the theoretical scattering function. [11] All the resultant values are in good agreement with each other suggesting the equality of the time and space self-similarity.

2. EXPERIMENTAL

Bovine fibrinogen (clottability 97%, Sigma-Aldrich Co.) was dissolved in a physiological saline solution (pH 7.4; 136.9 mM NaCl, 2.68 mM KCl, 1.47 mM KH_2PO_4 , 8.10 mM Na_2HPO_4) and this solution was dialyzed against the physiological saline solution overnight. Concentration of fibrinogen solution was determined from the absorbance at 280 nm, using an extinction coefficient of 1.51 ml/mg-cm. Thrombin (Mochida Co., Japan) solution was also prepared in the physiological saline solution. Fibrinogen solution was prepared to make a final concentration of 2.2 mg/ml, and the final thrombin concentration was 0.02 (sample A) and 0.00125 NIH units/ml (sample B).

Dynamic light scattering measurements were carried

out using a homemade spectrometer and an ALV-5000 multiple-tau digital correlator to obtain the correlation function of scattered light $g^{(2)}(t)$ and the averaged scattered light intensity simultaneously. The decay time distribution function $\tau G(\tau)$ was obtained from $g^{(2)}(\tau)$ by using CONTIN program. Light source was Ar ion laser with the wavelength $\lambda = 488$ nm and the details of the apparatus was described elsewhere [12]. Measurements of $g^{(2)}(\tau)$ in the time course of gelation were carried out at the scattering angle of 30° and were obtained by the homodyne mode. All the measurements of light scattering were performed at 37°C .

CLSM was carried out by use of LSM510 (Carl Zeiss) using an Ar-ion laser as an excitation light source. Thoroughly gelled samples were treated by 0.17mM fluorescein isothiocyanate (FITC) solution. In order to prevent the photo-bleaching, 50mM of p-phenylenediamine was percolated to the fibrin gel. [13] The emission of 505-530nm from FITC was detected through a filter system, and 256 images stacked in every $0.1\mu\text{m}$ depth covering the observation area of $25.6 \times 25.6 \mu\text{m}$ with $0.05 \times 0.05 \mu\text{m}$ resolution. 256 sliced images were stacked and 3-D image was reconstructed. Resultant images were deconvoluted to remove the blurring effect. Eight sets of observations were averaged.

The CLSM image is not the fibrin fiber itself, but the fluorescence image of FITC bound to fibrin fibers. In fact, the fractal dimension obtained by the box-counting method depends on the threshold level. Therefore, a proper setting of the threshold level for the binarization of fluorescence intensity is necessary. Wave length dependence of the turbidity over 400 to 800 nm for the gelled samples was obtained and the fiber diameter was evaluated according to Carr et al. [14] Threshold level was determined so that the resultant average fiber diameter coincides with that determined by turbidity.

The network images thus binarized were analyzed at first by the box-counting method. 3-D images were divided into small cubes of size R , and the number of the cubes that contains any part of the network, $N(R)$, was counted. When the spatial self-similarity holds,

$$N(R) \sim R^{-D_f}$$

is realized, and D_f is the fractal dimension. When cube size is smaller than one pixel and larger than the image size (512 pixels), box counting must give 3 dimensional behavior ($D_f = 3$) Therefore, the double logarithmic plots of $N(R)$ against R at the both extremes should be expressed by the lines with the slopes of -3 .

Power spectra of the 3-D images were obtained by means of fourier transform, and are related to the scattering function with equating the absolute magnitude of the spatial frequency to the scattering vector. [15]

3. RESULTS AND DISCUSSION

Figure 1 shows the temporal growth of the correlation function of the sample B. The overall characteristics are essentially the same for the sample A except for the elapsed time. At the elapsed time larger than 237 min, very slow tailing of the correlation function becomes remarkable. At 260 and 286 min, power law behavior is observed. At 286 min the initial amplitude decreased definitely. It results from the decrease of coherence due to the restricted ergodicity by the frozen homogeneity. That is, gelation occurs already at 286 min. After the

gelation occurred, the overall behavior of the correlation function is almost the same except for the marked decrease of the initial amplitude. This fact suggests that the temporal self-similarity is essentially unchanged even at the post gel state.

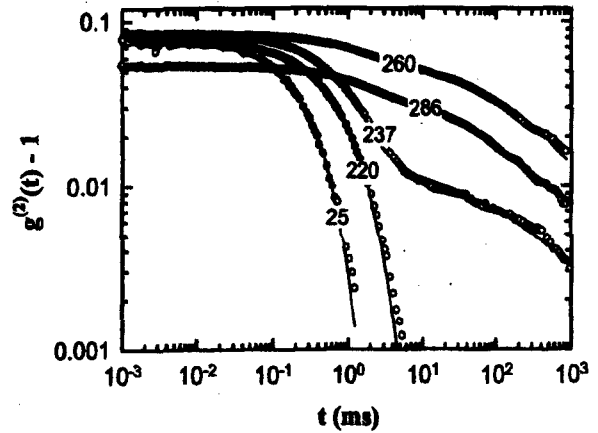


Fig. 1. Time evolution of the correlation function of the sample B at the scattering angle 30° . Numerical values for the curves denote the elapsed time. Power law behavior was observed at 260 and 286 min.

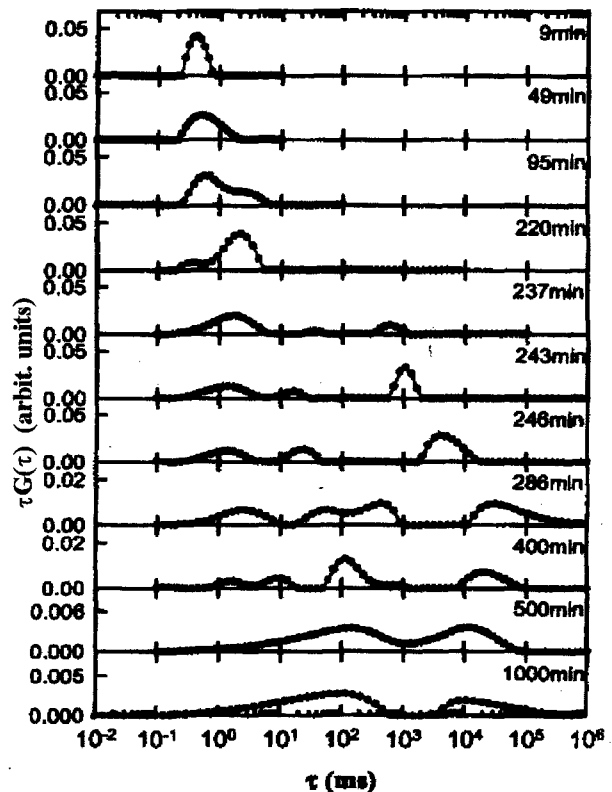


Fig. 2. Temporal evolution of the decay time distribution $\tau G(\tau)$ of the sample B. Gelation time is 270-286 min. The conversion process of fibrinogen to protofibril is clearly demonstrated in the time range until 220 min.

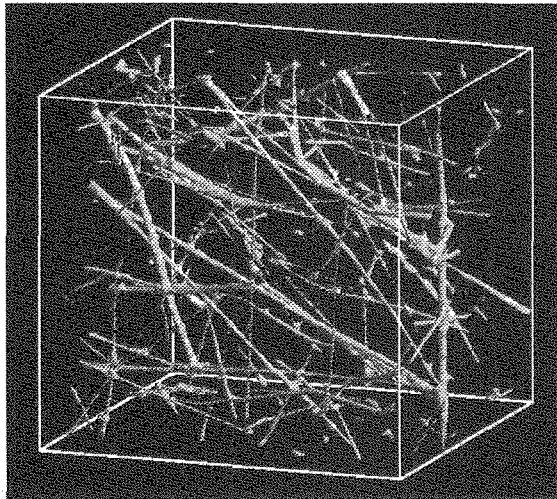


Fig. 3. 3-D network image of fibrin gel reconstructed from the stacked 2-D slice images by CLSM of the sample A. The length of each side is 25.6 μm .

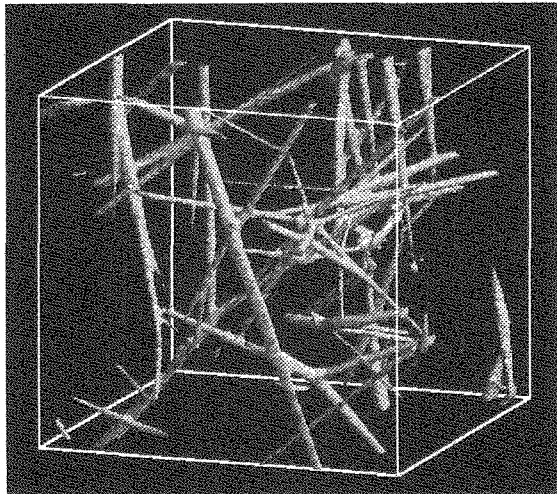


Fig. 4. 3-D network image of fibrin gel reconstructed from the stacked 2-D slice images by CLSM of the sample B. The length of each side is 25.6 μm .

Figure 2 shows the time course of the decay time distribution function $\tau G(\tau)$ for the sample B. For the elapsed time smaller than 220 min, decay time distributes in relatively short time range, which corresponds to fibrinogen, fibrin monomer, and protofibrils. Protofibril formation is shown by the appearance of intergradations of the decay modes at ca. 1 ms. In fact, in this time range the relationship between the averaged decay time and the scattered intensity is represented by a linear relation, which means the axial (staggered) growth of fibrin molecules. At 237 min, slow decay mode appears around at 1s accompanied with rapid increase of scattered light intensity and those modes correspond to the lateral growth and network (branching) formation. With the growth of such a slow decay mode, very slow decay mode $>$ ca. 10 s appears at 286 min, and the decay time distribution becomes to span over very wide range. After 286 min, fast decay mode becomes weakened. It is related to the cooperative diffusion of gel network and the weak intensity correlates to the stiffness of chains between the crossbridging points (regions).

Martin et al first reported the fractal dimension of gels deduced from the power law behavior of the correlation function. [6] Self-similar structure realized in the percolated gel network results in equally the self-similar fluctuating behavior, and thus the exponent of power law correlates to the fractal dimension. According to Muthukumar, $1 - \phi = d(d + 2 - 2D_f)/2(d + 2 - D_f)$ with ϕ being the exponent of power law relation of correlation function and d the spatial dimension ($= 3$). [5] Samples A and B give $\phi = 0.093$ and 0.16 , and $D_f = 1.42$ and 1.53 , respectively. [3] These values are quite smaller than those predicted for the gel of flexible chains (2.0-2.5). Smaller D_f is obtained for the sample A where the faster gelation occurs with higher thrombin concentration.

In order to examine the applicability and the equality of spatial and temporal self-similarity, the real space observation of fibrin gel was carried out using CLSM. Typical images reconstructed from the slice images are shown in Figs. 3 and 4. Network structure of fibrin gel is clearly observed, and the respective fibrin fibers constructing network is definitely visible. CLSM images

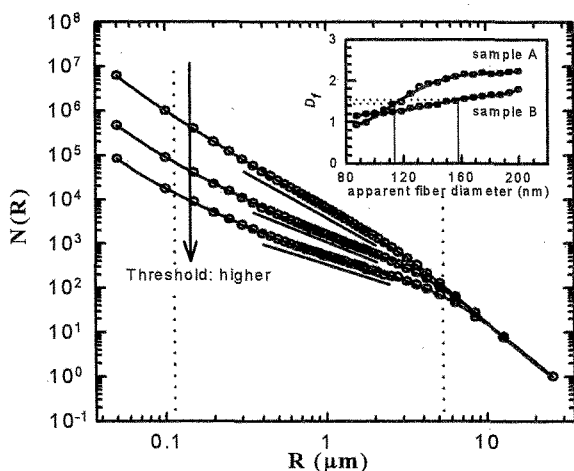


Fig. 5. Threshold level dependence of the relationships of $N(R)$ vs R in the box-counting method.

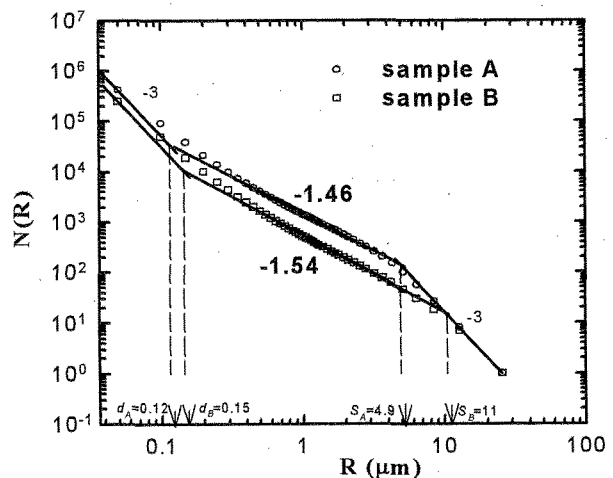


Fig. 6. Double logarithmic plots of $N(R)$ vs R . In the central region linearity holds well.

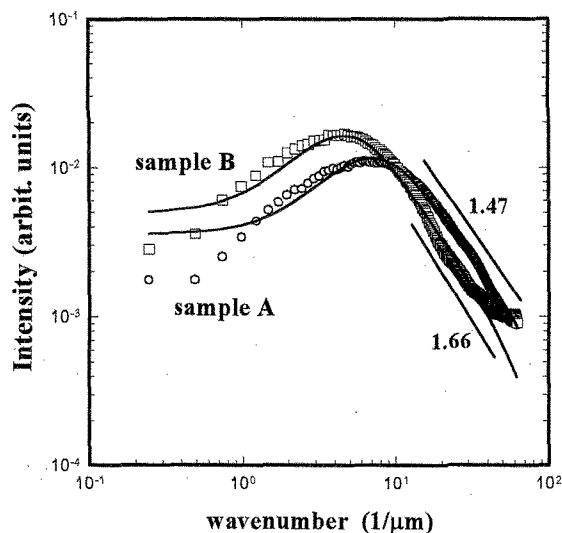


Fig. 7. Power spectra obtained by 3-D fourier transform of CLSM image. The solid curves are the fitted ones.

are the fluorescence images of FITC bound to fibrin. In order to perform the box-counting method for the analyses of network structure and the determination of fractal dimension, binarizing the observed images with appropriate threshold level is necessary. Figure 5 shows the threshold level dependence of $N(R)$ and D_f . The correct level was determined by the procedure that the average fibrin fiber diameter constituting gel network obtained at a threshold level should coincide with that determined by turbidity measurement (113 and 157 nm for the samples A and B, respectively). Figure 6 is the resultant relationships of $N(R)$ vs R by box-counting method for the samples A and B. In the central region, linear relation between $N(R)$ and R holds well suggesting the self-similar network structure. The resultant slopes D_f are 1.46 and 1.54 for the sample A and B, respectively. These values are in good accordance with those obtained by light scattering. The relationship of $N(R)$ vs R must have the slope of -3 where R is below one pixel and above image size, and then the straight lines of slope -3 passing the data points of $R = 0.05$ and $25.6 \mu\text{m}$ were drawn. Those two lines cross the regression lines for the central region, and the crossing points are regarded as the average fiber diameter and the characteristic mesh size of the network. The evaluated magnitudes were 0.12 and $0.15 \mu\text{m}$ for the diameter and 4.9 and $11 \mu\text{m}$ for the characteristic mesh size for the sample A and B, respectively. Diameters determined by turbidity are 0.11 and $0.16 \mu\text{m}$, and they are in good agreement indicating the proper box-counting treatments. Larger mesh size in the sample B with slow gelation process means the sparse network with more grown fibrin fibers laterally. Lateral growth of fibrin fibers in the sample B yields broader (or heterogeneous) distribution. This is the reason why the fibrin gel with low thrombin concentration generally gives high turbidity.

In order to verify the validity of the fractal dimension further, the power spectra were obtained by 3-D fourier transform of the CLSM images. Figure 7 illustrates such plots. The appearance of the peak means the existence of characteristic length in accordance with the mesh size. Power law behavior of the spectra is observed in the

wavenumber region greater than the peak. The slope corresponds to the fractal dimension, and $D_f = 1.47$ and 1.66 were determined. Of course, these values are in good agreement with those determined by box-counting.

The solid curves in Fig. 7 are the fitted ones derived by Ferri et al, and a sufficiently good fitting is obtained. [11] Their formulation assumes the self-similar structure and the scattering function are composed of two factors, a structure factor describing the correlation between the blobs (corresponding to mesh size) and a form factor describing the internal structure of the blob (inside the mesh). Spatially self-similar structure is characterized mainly by the form factor with fractal dimension. Full description of the scattering function is described elsewhere. As shown in Fig. 7, the fitting is sufficient and the resultant fractal dimension was 1.40 and 1.53 and the blob size was evaluated as 3.61 and $5.34 \mu\text{m}$ for the sample A and B, respectively. All the evaluated values of fractal dimension are consistent with each other: light scattering, box-counting, power spectrum, and fitting to theoretical formulation. The equality between the spatial and temporal (decay time of density fluctuation) self-similarity holds well. The utilization of Muthukumar's equation for the gels composed of stiff chains (e.g., gellan gum) could be safely carried out.

In conclusion, gelation process of fibrin gel was characterized by time-resolved light scattering measurement, and the self-similar characteristics of fibrin gel were ascertained using fractal dimension by means of CLSM. Various methods to evaluate the fractal dimension exhibit good agreement with each other.

REFERENCES

- [1] R. Hantgan, W. Fowler, H. Erickson and J. Hermans, *Thromb. Haemost.*, 19, 119 (1980).
- [2] E. Regañón, V. Vila and J. Aznar, *Haemostasis*, 14, 170 (1984).
- [3] R. Kita, A. Takahashi, M. Kaibara and K. Kubota, *BioMacromolecules*, 3, 1013 (2002)
- [4] D. Stauffer, *J. Chem. Soc. Faraday Trans.*, 272, 1354 (1976)
- [5] M. Muthukumar, *Macromolecules*, 22, 4656 (1989).
- [6] J. E. Martin and J. P. Wilcoxon, *Phys. Rev. Lett.*, 61, 373 (1988).
- [7] Y. Hirokawa, H. Jinnai, Y. Nishikawa, T. Okamoto and T. Hashimoto, *Macromolecules*, 32, 7093 (1999).
- [8] B. Blomback, K. Carlsson, B. Hessel, A. Liljeborg, R. Procyk and N. Aslund, *Biochimica Biophysica Acta*, 997, 96 (1989).
- [9] J. D. Farmer, E. Ott, and J. A. Yorke, *Physica D*, 7, 153 (1983).
- [10] H. Tanaka, T. Hayashi and T. Nishi, *J. Appl. Phys.* 59, 3627 (1986).
- [11] F. Ferri, M. Greco, G. Arcovito, F. A. Bassi, M. DeSpiriti, E. Paganini and M. Rocco, *Phys. Rev. E*, 63, 31401 (2001).
- [12] K. Kubota, H. Urabe, Y. Tominaga and S. Fujime, *Macromolecules*, 17, 2096 (1984).
- [13] J. L. Platt and A.F. Michael, *J. Histochem. Cytochem.*, 31, 840 (1988).
- [14] M. E. Carr, Jr. and J. Hermans, *Macromolecules*, 11, 46 (1978).
- [15] A. Takahashi, R. Kita, T. Shinozaki, K. Kubota and M. Kaibara, *Colloid Polym. Sci.*, in press (2002).